Electronic Supplementary Information

Phonons and Excitons in $ZrSe_2$ - ZrS_2 Alloys

Sean M. Oliver,[a,b] Joshua J. Fox,[c,d], Arsalan Hashemi,[e] Akshay Singh,[f,g] Randal L. Cavalero,[c,d] Sam Yee,[a,b] David W. Snyder,[c,d] R. Jaramillo,[f] Hannu-Pekka Komsa,[e,h] and Patrick M. Vora*[,a,b]

[a] Department of Physics and Astronomy, George Mason University, Fairfax, VA, USA
[b] Quantum Materials Center, George Mason University, Fairfax, VA, USA
[c] Electronic Materials and Devices Department, Applied Research Laboratory, Pennsylvania State University, University Park, Pennsylvania, USA
[d] 2-Dimensional Crystal Consortium, Materials Research Institute, Pennsylvania State University, University Park, Pennsylvania, USA
[e] Department of Applied Physics, Aalto University, Aalto, Finland
[f] Department of Materials Science and Engineering, Massachusetts Institute of Technology, Cambridge, MA, USA
[g] Department of Physics, Indian Institute of Science, Bangalore, India
[h] Microelectronics Research Unit, University of Oulu, Oulu, Finland

* E-mail: pvora@gmu.edu

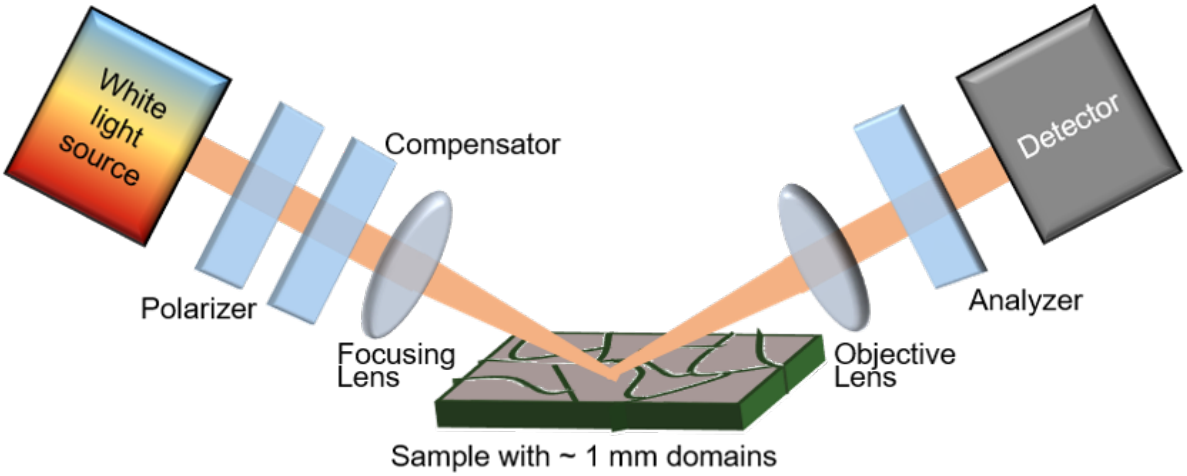

Figure S1: Schematic of M-2000 Woollam instrument used for spectroscopic ellipsometry. The light is focused on the sample to a spot size of ≈300 µm. The data is taken from flat and reflective domains (≈1 - 3 mm) on the freshly-exposed basal face of the crystals.

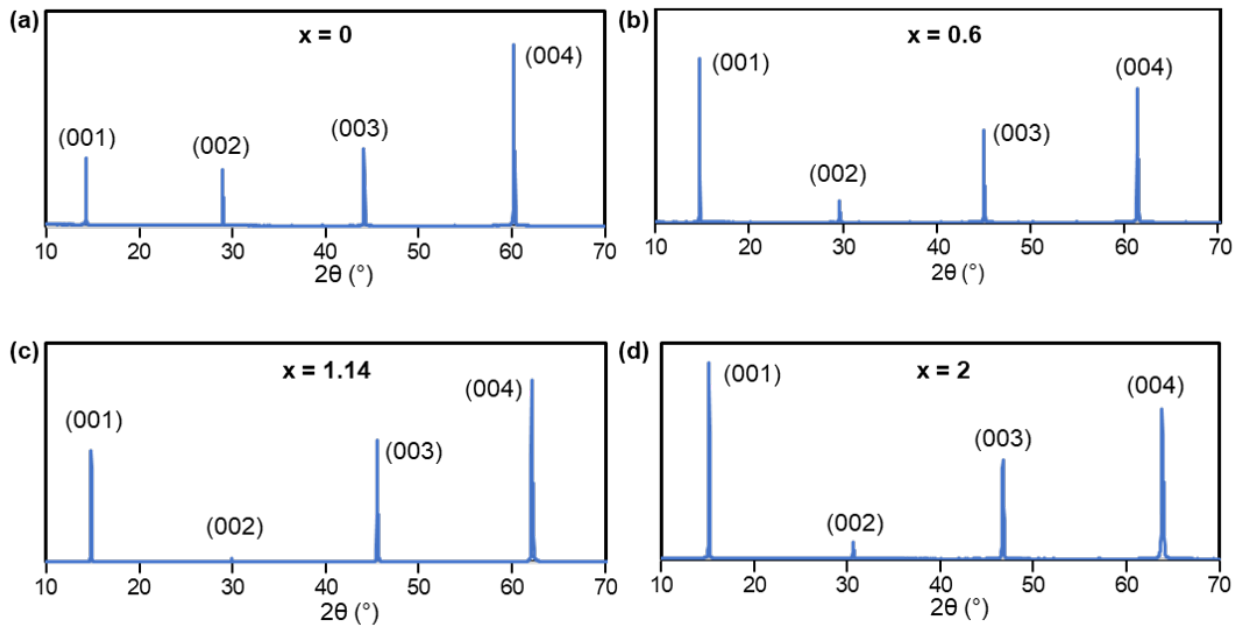

Figure S2: X-ray diffraction (XRD) measurements for select members of the ZrS_xSe_{2-x} alloy family corresponding to (a) $ZrSe_2$ (x = 0), (b) x = 0.6, (c) x = 1.14, and (d) ZrS_2 (x = 2). 2θ scans show a single-phase, c-axis oriented, layered crystal across the entire alloy compositional range displaying reflections of $(00l)$ peaks in the scan range for $l = 1$, 2, 3, and 4.

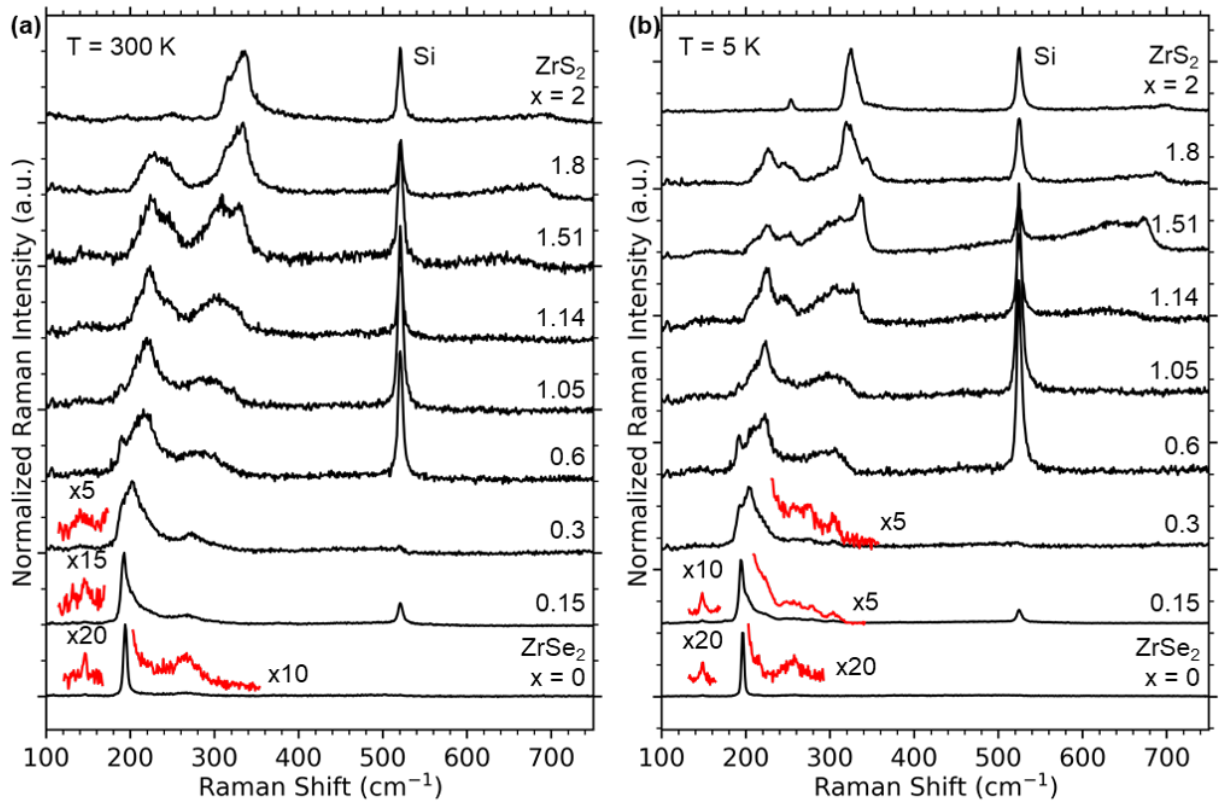

Figure S3: Unpolarized Raman spectra of the ZrS_xSe_{2-x} alloys taken at (a) 300 K and (b) 5 K with 532 nm excitation. Portions of the spectra have been scaled for clarity (red curves). The large feature at ≈520 cm^{-1} is from the Si substrate.

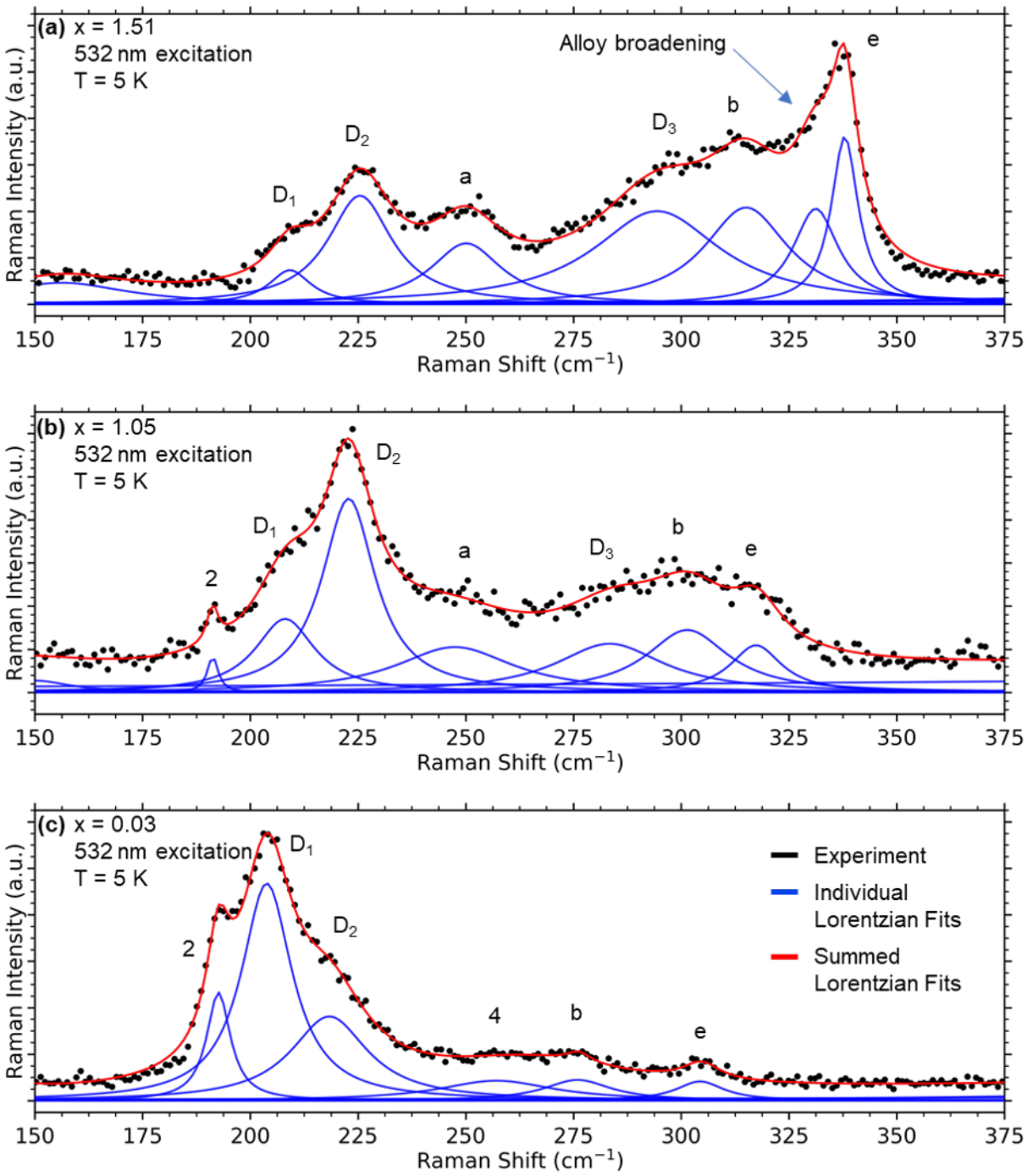

Figure S4: Unpolarized Raman spectra demonstrating Lorentzian fits to select ZrS_xSe_{2-x} alloys corresponding to (a) x = 1.51, (b) x = 1.05, and (c) x = 0.03. The black points are experimental data, the blue curves are individual Lorentzian fits, and the red curves are the total fits determined by summing the individual Lorentzian fits. The spectra are labeled with the letters and numbers shown in Figure 3a of the main text. Measurements are taken at 5 K with 532 nm excitation.

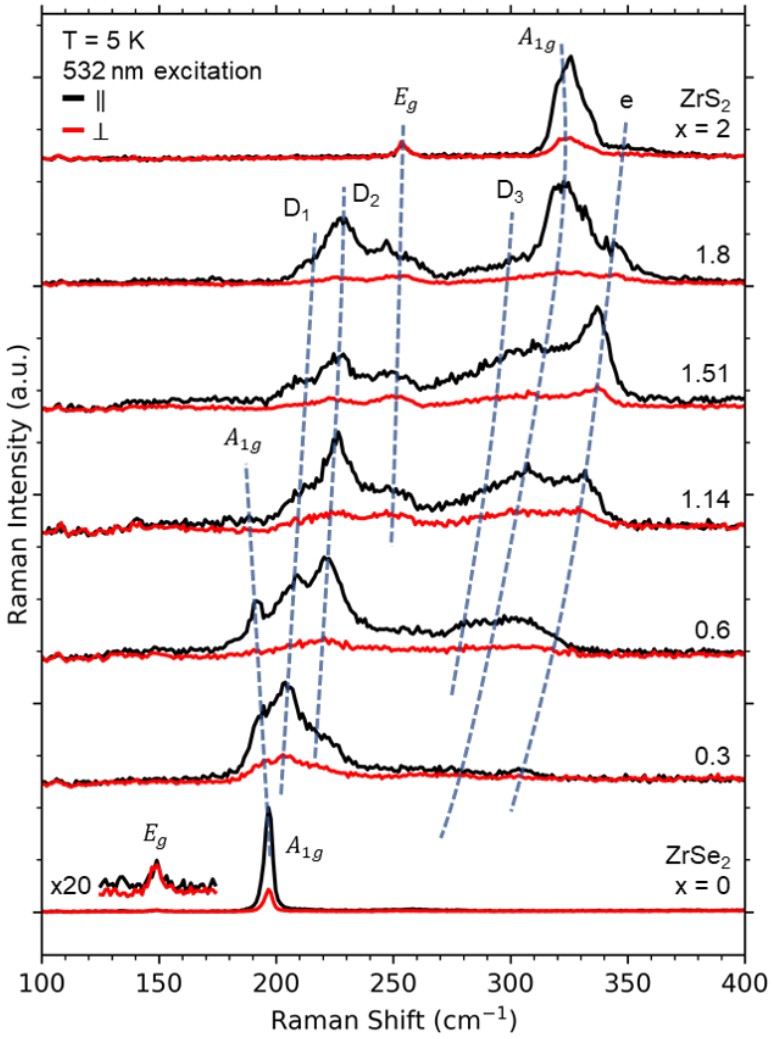

Figure S5: Polarization-resolved Raman spectra of ZrS_xSe_{2-x} alloys taken at 5 K with 532 nm excitation. The black and red curves are taken with the polarization axis of the excitation laser and the analyzing polarizer aligned either co-polarized (‖) or cross-polarized (⊥), respectively. The E_g mode in $ZrSe_2$ (x = 0) has been scaled for clarity. Dashed lines are drawn to illustrate the evolution of some of the most prominent vibrational modes with alloying. The peak labels are the same as those found in Figures 3a and 3b of the main text.

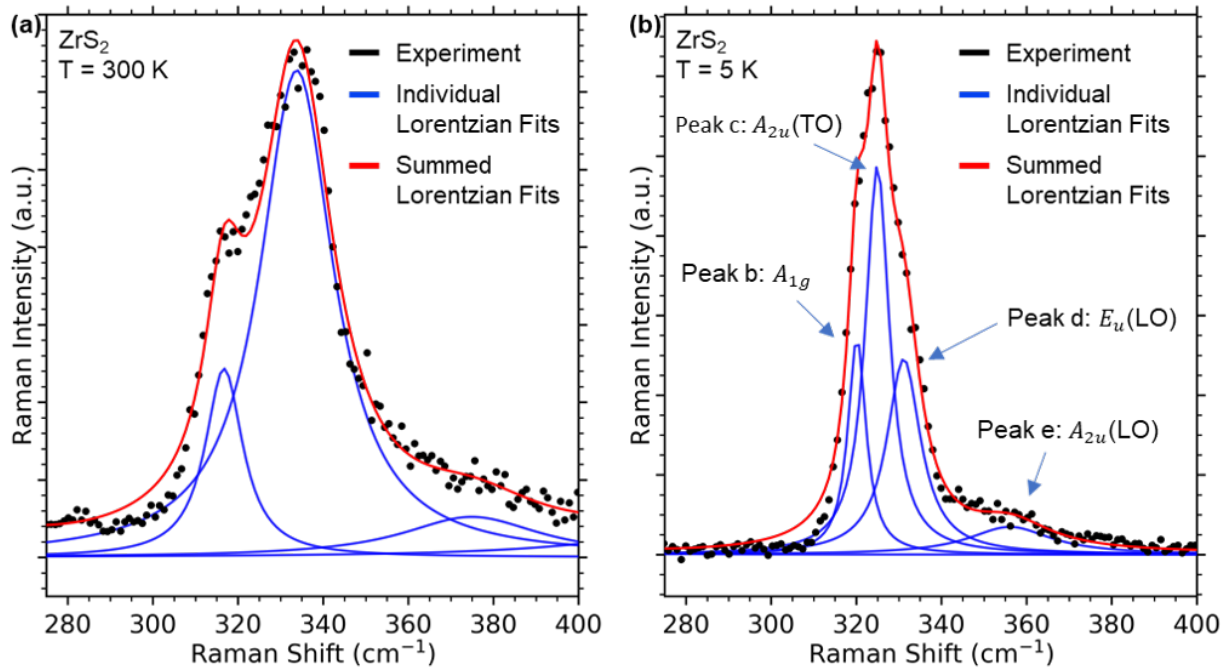

Figure S6: Unpolarized Raman spectra of ZrS_2 taken at (a) 300 K and (b) 5 K with 532 nm excitation and centered on the broad peak at ≈330 cm^{-1}. The black points are experimental data, the blue peaks are individual Lorentzian fits, and the red curves are total fits determined by summing the individual Lorentzian fits. At 300 K, there is significant thermal broadening of the large peak at 334 cm^{-1}. The fine structure of the features in this frequency range are revealed when we cool ZrS_2 to 5 K, which otherwise is masked by thermal broadening at elevated temperatures. We find at 5 K that these features are best fit with three Lorentzian peaks, which are determined to be the primary ZrS_2 A_{1g} mode (peak b) hybridized with IR modes labeled peaks c and d. There is also a weak, higher energy feature labeled peak e that is assigned to an IR phonon. The peak labels, which are the same letters used in Figures 3a and 3b of the main text, are accompanied by their respective symmetry assignments.

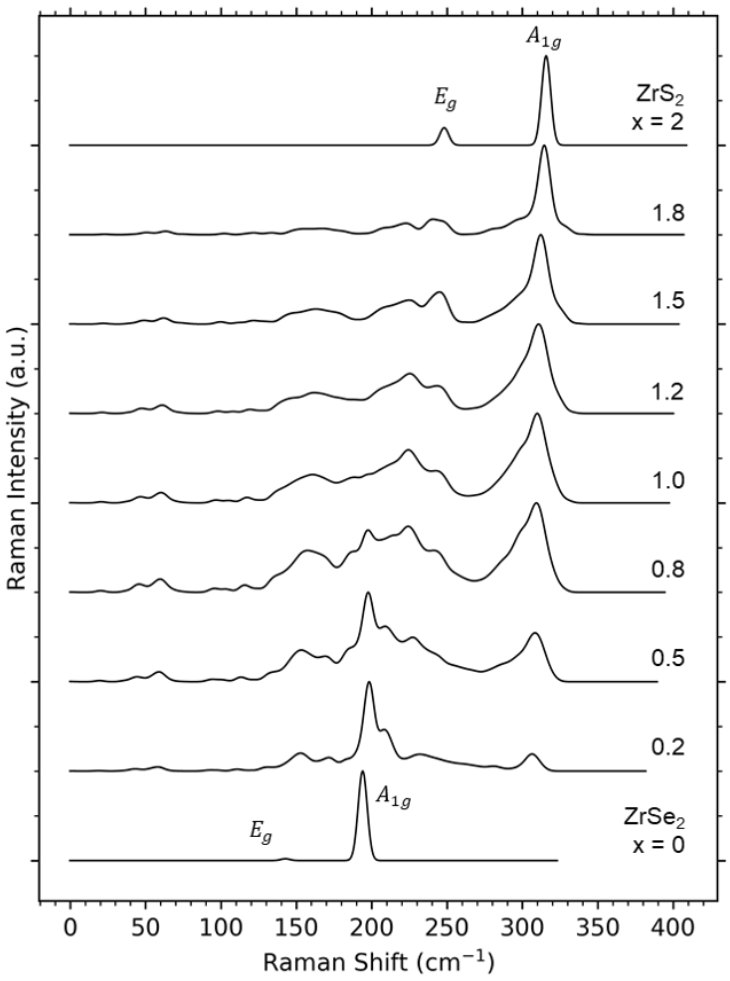

Figure S7: Simulated Raman spectra for ZrS_xSe_{2-x} alloys across the entire compositional range. See the *Experimental and Theoretical Methods* section of the main text for details on these simulations. The spectra have been offset vertically for clarity.

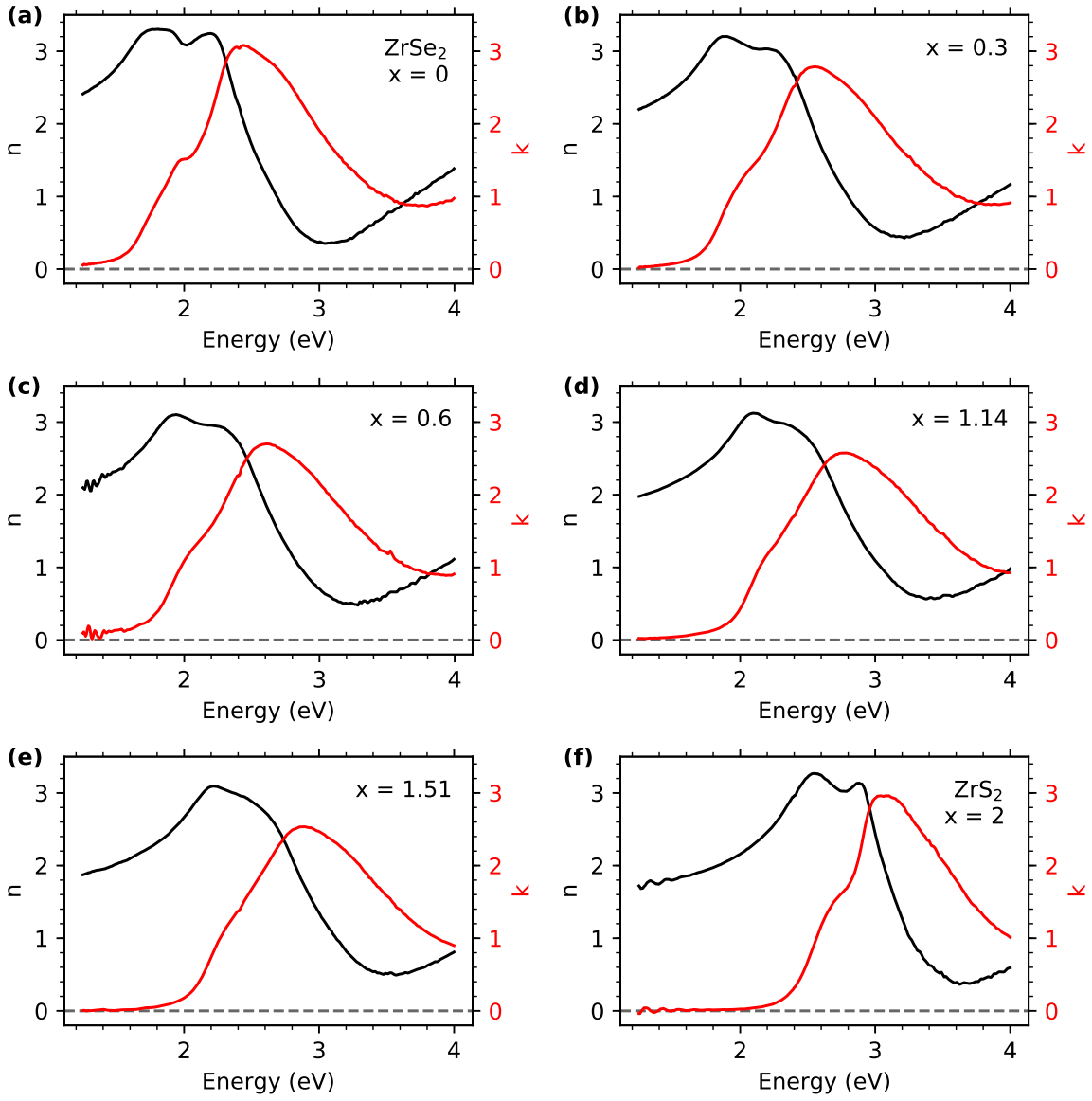

Figure S8: Optical constants measured by spectroscopic ellipsometry of ZrS_xSe_{2-x} alloys at room temperature. Real components (n, black curves, left axes) and imaginary components (k, red curves, right axes) of the complex refractive index for compositions (a) x = 0, (b) x = 0.3, (c) x = 0.6, (d) x = 1.14, (e) x = 1.51, and (f) x = 2.

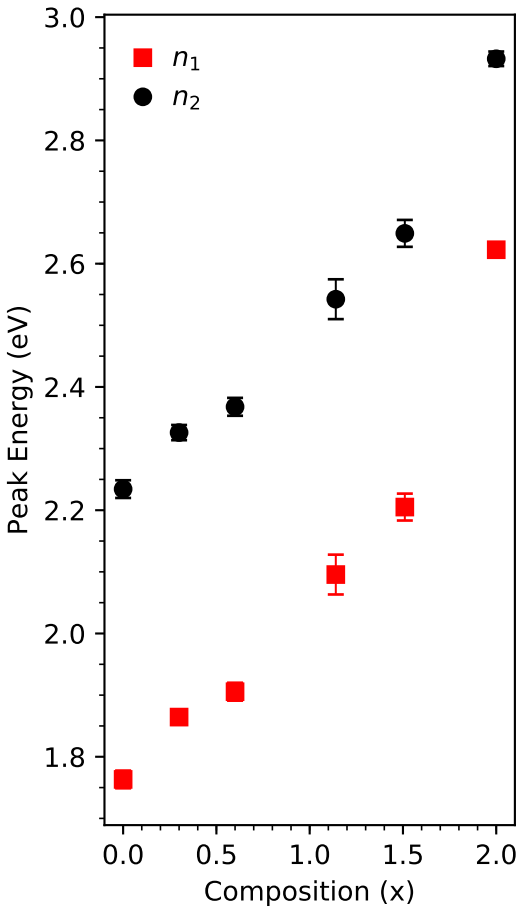

Figure S9: Peak energies extracted from Voigt fitting to the real components of the complex refractive index (n) obtained from spectroscopic ellipsometry measurements at room temperature. The labels n_1 and n_2 refer to the lower energy peak and the higher energy peak in Figure 5 of the main text, respectively.

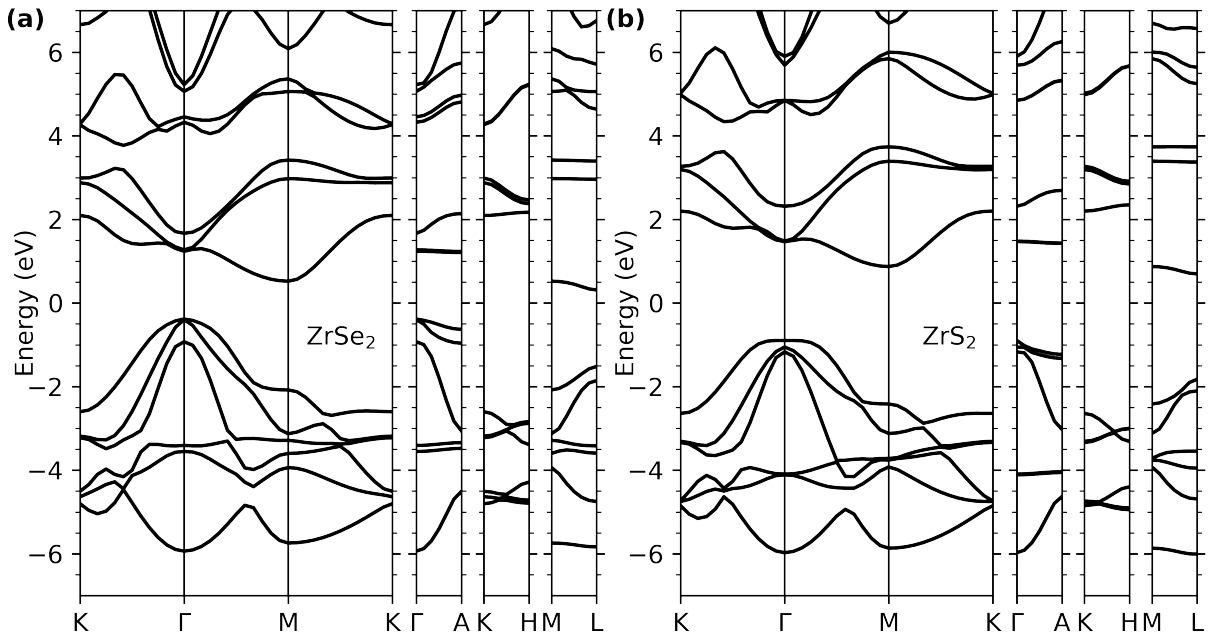

Figure S10: Electronic band structures of (a) $ZrSe_2$ and (b) ZrS_2.